ELSEVIER

Journal of Alloys and Compounds 275–277 (1998) 186–190

Journal of ALLOYS AND COMPOUNDS

Photon avalanche upconversion in various Tm^{3+}-doped materials

S. Guy, M.-F. Joubert*, B. Jacquier

Laboratoire de Physico-Chimie des Matériaux Luminescents, UMR CNRS 5620, U. Lyon 1, 69622 Villeurbanne Cedex, France

Abstract

We demonstrate the good agreement between theory and experimental results concerning the effect of the rare-earth ion concentration, the metastable state lifetime and the nonresonant ground state absorption cross section on the photon avalanche efficiency. © 1998 Elsevier Science S.A.

Keywords: Nonlinear processes; Photon avalanche; Tm^{3+} spectroscopy; Upconversion

1. Introduction

Among the upconversion mechanisms which give rise to fluorescence at higher frequency than that of excitation light, the photon avalanche leads to strong upconverted emission even without resonant ground state absorption (GSA). The pump photon energy is only resonant between a metastable state and a higher level of the active ion. The main characteristic of such a process is an excitation power threshold which corresponds to a sudden absorption of the pump photons and, therefore, to a sudden increase of the upconverted fluorescence; at the same time, there is a slowing down and change of the rise shapes of the transient signals.

Since its discovery in Pr^{3+}-doped materials [1], the photon avalanche has been observed in many other rare-earth-doped materials. In the present work, we show that the efficiency of the photon avalanche depends on three fundamental parameters: the cross relaxation rates, the ratio of the nonresonant GSA to the resonant excited state absorption (ESA) cross sections and the metastable state lifetime. Experimentally, we can act on these parameters by using different rare-earth concentrations, different excitation wavelengths or different hosts for the active ion.

We present experimental results obtained with different Tm^{3+}-doped materials ($YLiF_4$ (YLF), $Y_3Al_5O_{12}$ (YAG) and $YAlO_3$ (YAP) single crystals and BIGaZYTZr fluoride glasses) in which photon avalanche leads to intense blue emission after red CW pumping. The effect of the three fundamental parameters is then clearly established as predicted by the mean field theory.

*Corresponding author. Tel.: +33 4 72 44 83 39; fax: +33 4 72 43 11 30; e-mail: joubert@pcml.univ-lyon.fr

0925-8388/98/$19.00
PII: S0925-8388(98)00300-4

2. Theoretical description

The microscopic mechanism responsible for the self storage of the metastable state has been identified [1]. Concerning the macroscopic description, as the photon avalanche is a bifurcation, the mean field approach is valid to describe this process and, effectively, it has been shown that the rate equation model reproduces quantitatively the experimental results as soon as the Gaussian intensity profile of the input beam is taken into account [2]. The main characteristic of the photon avalanche is an excitation intensity threshold and its signature is a slowing down of the transient fluorescence signal at threshold. Therefore, the significant spectroscopic parameters for photon avalanche can be found by analysing the theoretical expressions of these two quantities.

2.1. The excitation intensity threshold

The theoretical expression for the excited state pumping rate threshold R_{2th} shows clearly that the cross relaxation energy transfer rate (s) involved in populating the metastable state should be high enough for this threshold to exist [2]. Then R_{2th} is the value from which the self storage of the metastable state becomes more efficient than the losses. As the cross relaxation energy transfers are due to interactions between the active ions, the rare-earth ion concentration is a critical parameter for the avalanche to occur. Moreover, the metastable state lifetime τ_2 is inversely proportional to R_{2th} [2]. Therefore, a long metastable state lifetime will favour a low excited state pumping rate threshold. On the other hand, the excitation intensity at threshold is given by [2]

$$I_{th} = \frac{R_{2th}/\sigma_2}{1 - bR_{2th}\tau_2\sigma_1/\sigma_2}$$

where σ_2 is the ESA cross section, σ_1 is the cross section of the residual GSA and b is a function of the relaxation rates of the higher energy levels of the system. So a high σ_2 also favours a low excitation intensity threshold. The increase of I_{th} with the GSA cross section σ_1 is not significant as soon as σ_1 is more than one order of magnitude lower than σ_2.

2.2. The critical slowing down at threshold

At threshold, the time to reach the stationary solution is maximum. Assuming quasi-equilibrium of higher excited levels with the metastable level, such an adiabatic approximation being correct below and around the threshold, we showed that the absorption and fluorescence dynamics present an hyperbolic tangent profile [2]. We obtained a theoretical expression of the characteristic time at threshold which is proportional to the time of establishment τ_e (time for which the fluorescence reaches 99% of its stationary value). It appears that the critical slowing down, which is the ratio of τ_e to the metastable state lifetime τ_2, is proportional to [2]

$$\sqrt{\frac{\sigma_2}{\tau_2\sigma_1}}$$

Then, the slowing down at threshold, which is the signature of photon avalanche, depends heavily on τ_2 and σ_1/σ_2: the lower τ_2 and σ_1/σ_2, the more the slowing down should be spectacular. However, as discussed above, the intensity threshold increases if τ_2 decreases.

3. Experimental results and discussion

Numerous photon avalanche observations have been reported up to room temperature in Tm^{3+}-doped compounds leading to the strong blue emission ($^1G_4 \rightarrow {}^3H_6$) of Tm^{3+} after red excitation pumping resonant with the $^3F_4 \rightarrow {}^1G_4$ transition [3–8]. The experimental results presented in this section have been chosen to emphasize the effect of the three main parameters discussed in Section 2.

3.1. Active ion concentration effect

As already mentioned, the rare-earth ion concentration should be high enough for the photon avalanche to occur. However, for too high Tm^{3+} concentrations, the upconverted fluorescence is quenched; moreover, the metastable state lifetime may decrease, leading to an increase of the photon avalanche threshold. The optimum doping level will, therefore, be a compromise between these competing concentration behaviours.

Table 1
Comparison of the photon avalanche experimental results for Tm^{3+}-doped BIGaZYTZr glasses containing $30BaF_2$, $18InF_3$, $12GaF_3$, $20ZnF_2$, $6ThF_4$, $4ZrF_4$, $(10-x)YF_3$ and $xTmF_3$ under 649 nm excitation at 100 K

	$x=1$ mol%	$x=3$mol%	$x=7$ mol%
$\eta(s_4)$ (%)	77	97	99.7
$\eta(s_3)$ (%)	58	94	99
τ_2 (ms)	13	9.3	1
I_{th} (kW cm^{-2})		9.5	
n_{th}		4	
τ_e/τ_2		11.4	
σ_2 (10^{-20} cm^2)		0.28	
σ_1/σ_2		12×10^{-3}	

An illustration of this concentration effect is shown in Table 1, related to Tm^{3+}-doped BIGaZYTZr fluoride glasses. Spectroscopic measurements lead to the metastable state lifetimes τ_2 and cross relaxation quantum yields ($\eta(s_3)$,$\eta(s_4)$) given in Table 1. The cross relaxation rates are small in the 1 mol% doped glass, more efficient in the 3 mol% doped glass and very efficient in the 7 mol% doped glass in which the energy transfer quantum yields are about 100%. As shown in Fig. 1, we observed photon avalanche behaviour in the 3 mol% doped glass: the upconverted fluorescence intensity increases with a slope of 4 ($n_{th}=4$) at the threshold and the critical slowing down is 11.4. In the 1 mol% doped glass, the cross relaxation rates are not sufficient, so the blue emission exhibits a quadratic excitation power dependence (characteristic of a two step absorption process) whatever the excitation power. In the 7 mol% doped glass, due to the lower value of τ_2 and to the higher efficiency of the cross relaxation energy transfers, the blue fluorescence is extremely small over all the excitation power range.

3.2. The metastable state lifetime

Photon avalanche red to blue upconversion was observed in Tm^{3+}-doped YAP or YAG at room temperature. Table 2 shows a comparison of the experimental results obtained for YAP: 3.6 at% Tm^{3+} and YAG: 5 at% Tm^{3+}. In these two crystals, the cross relaxation quantum yields are about the same, but the $^3F_4$ lifetime is significantly different. By fitting the photon avalanche experimental transient curves, it appears that the absorption cross section ratios are equal. So, these two examples are nice for checking the influence of the metastable state lifetime. At threshold, the blue fluorescence increases with a slope of >7 and the critical slowing down is 35 in the YAP crystal, these parameters being only 3 and 19, respectively, in the YAG crystal. So, it is clear that the photon avalanche is more spectacular in the sample which has the lower τ_2 value. Moreover, the proportionality between the slowing down and $\tau_2^{-1/2}$ predicted by the theory is verified.

Another interesting example is the comparison between the red to blue photon avalanche results obtained with

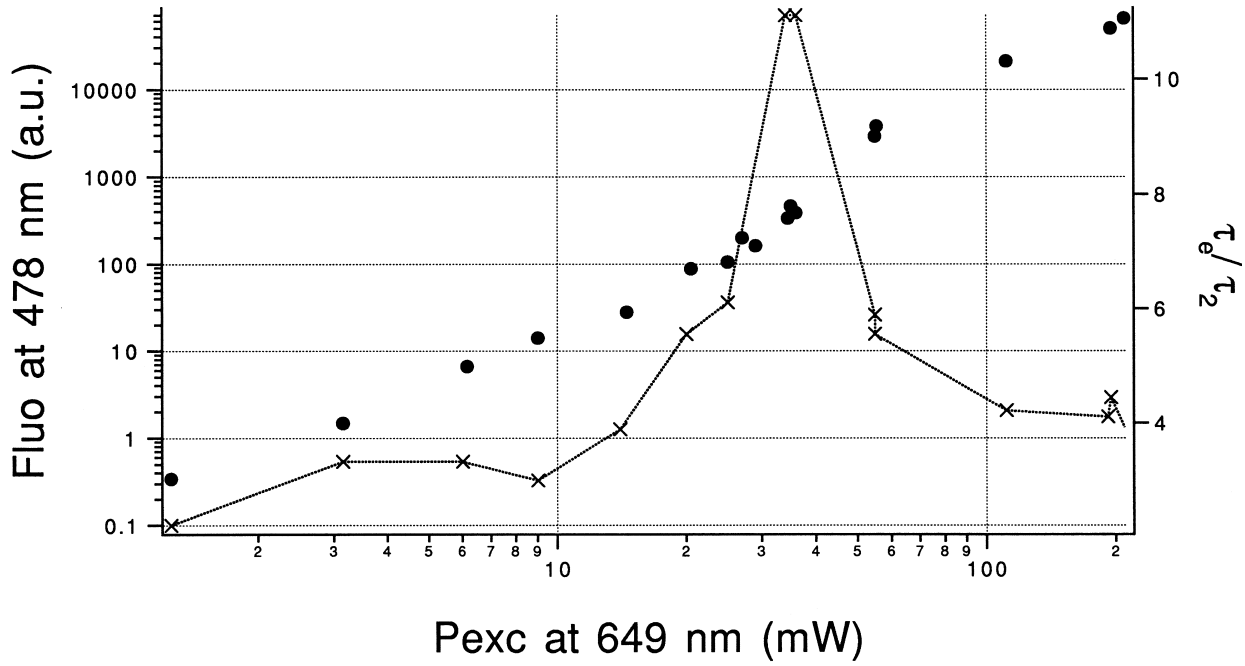

Fig. 1. Experimental variation of the stationary upconverted fluorescence intensity (●) and of the slowing down (×) versus the excitation power in the 3 mol% Tm^{3+}-doped BIGaZYTZr glass at 100 K.

Table 2
Comparison of the photon avalanche experimental results for YAP: 3.6 at% Tm^{3+} and YAG: 5 at% Tm^{3+} at room temperature

	YAP (exc: 638 nm)	YAG (exc: 617 nm)
$\eta(s_4)$ (%)	85	94
$\eta(s_3)$ (%)	94	96
τ_2 (ms)	2.85	8.5
R_{2th} (s^{-1})	227	65
I_{th} (kW cm^{-2})	6.06	6.5
n_{th}	7–8	3–4
τ_e/τ_2	35	19
σ_2 (10^{-20} cm^2)	1.1	0.32
σ_1/σ_2	2×10^{-3}	2×10^{-3}

YLF: Tm^{3+} samples (see Table 3). For the 5 and 10 at% doped crystals, we used the same excitation wavelength (647.9 nm), so the σ_1/σ_2 are identical. The cross relaxation quantum yields evaluated from the experimental decay curves under pulsed laser excitation are about the same, but the metastable state lifetimes are quite different. The

Table 3
Comparison of the photon avalanche experimental results for YLF: 5 at% Tm^{3+} and YLF: 10 at% Tm^{3+} under 647.9 nm excitation at room temperature

	YLF: 5 at% Tm^{3+}	YLF: 10 at% Tm^{3+}
$\eta(s_4)$ (%)	97.5	99.6
$\eta(s_3)$ (%)	96	99.6
τ_2 (ms)	15.8	6.2
I_{th} (kW cm^{-2})	2.25	5.25
n_{th}	7.5	9
τ_e/τ_2	25	38

n_{th} and τ_e/τ_2 values given in Table 3 show clearly that the photon avalanche is more spectacular in the YLF: 10 at% Tm^{3+} sample, which has a τ_2 value more than two times lower than the YLF: 5 at% Tm^{3+} crystal. Moreover, as predicted by the theory, the experimental value of the excitation intensity at threshold is proportional to τ_2^{-1} and that of the slowing down at threshold is proportional to $\tau_2^{-1/2}$.

3.3. The effect of ground state absorption

In this subsection, we focus on the impact of the nonresonant GSA relative to the resonant ESA. First, from a theoretical point of view, it has recently been shown that avalanche pumping overcomes GSA as soon as the pumping intensity is above the avalanche threshold [2]. However, below threshold, GSA is the main pumping mechanism and reaches a dramatic enhancement at threshold. These characteristics are based on the fact that the photon avalanche process is a bifurcation phenomenon (second order phase transition) [2]. The ESA is the control parameter (analogue of the temperature for spin systems) and the GSA can be identified as an external field which reduces the difference between the two pumping regimes (two step absorption below the threshold and avalanche absorption above). Moreover, GSA significantly acts on the dynamics and the critical slowing down at threshold, which is an experimental signature of the photon avalanche, is proportional to $(\sigma_2/\sigma_1)^{1/2}$. So, as suggested previously [9], there is a limit value of σ_1/σ_2 above which the PA is no longer the main pumping channel for the upconverted fluores-

cence. That limit clearly depends on the spectroscopic characteristics of the rare-earth ion [2] which are associated with the host matrix and the rare-earth concentration in this host.

Experimental evidence for this can be seen by comparing Tm^{3+}-doped glasses and crystals. Glasses have broad absorption lines implying a significant overlap between GSA and ESA. Comparing Table 1 with Table 2 or Table 3 shows that the photon avalanche effect is much less significant for glasses: at threshold the critical slowing down of the establishment of the blue fluorescence is much smaller.

Another way to investigate the impact of GSA experimentally is to study the photon avalanche in the same sample for two different excitation wavelengths. This has been done for a 5 at% Tm-doped YAG crystal at 35 K. The crystal was pumped both at 638 and 617 nm. In this material, the ESA is less efficient at 638 nm than at 617 nm [10]; moreover, the excitation photon energy is closer to the GSA resonance for 638 nm than for 617 nm. So, we expect a higher σ_1/σ_2 ratio under 638 nm excitation. Indeed, by fitting the blue transient signals, we find 6×10^{-3} compared to 0.5×10^{-3} under 617 nm excitation. It is clear (see Table 4) that the lower σ_1/σ_2 ratio leads to more spectacular photon avalanche effects at threshold (higher τ_e/τ_2 and higher n_{th}). The proportionality between the slowing down and $(\sigma_2/\sigma_1)^{1/2}$ predicted by the theory is verified. Moreover, the excitation spectrum at an intensity far above the threshold shows that the upconverted fluorescence depends only on the ESA cross section and is not limited by the GSA cross section.

Finally, in order to measure the impact of the GSA more precisely, we introduce its ''susceptibility'' [2] as

$$\chi = \left(\frac{\partial n_2}{\partial R_1}\right)_{R_1\to 0}$$

where χ gives the variation of the metastable state population, n_2, due to the GSA at low pump intensity. If there is no avalanche, χ is proportional to the product of the GSA cross section and the effective lifetime. The lifetime decreases as the ESA increases. Thus, the susceptibility decreases with the ESA pump power. However, for the photon avalanche pumping, we have shown [2] that χ increases dramatically at the avalanche pumping threshold following the Curie law.

In order to measure χ, we used a 1.8 at% Tm: YLF single crystal for which there is also a strong avalanche effect under red 647.9 nm CW pumping, leading to strong blue fluorescence. All the following results were taken at room temperature. The dramatic enhancement of the blue upconverted fluorescence near the pump power threshold (10 mW) is shown in Fig. 2 as a dashed line. In order to measure the impact of the GSA, we pumped the sample with two beams: one, the ESA beam (647.9 nm), comes from a dye laser, and is resonant with the $^3F_4\to{}^1G_4$ transition. The other, the GSA beam (790 nm), is from a diode and is resonant with a transition from the ground state to the $^3H_4$ level. Both beams were focused into the sample with an achromatic lens of 76.2 mm focal length. We did not measure the overlap between the beams. The blue fluorescence was detected perpendicular to the pump beams via a monochromator and a photomultiplier. We measured the susceptibility of the GSA versus the upconverted fluorescence by comparing the signal with the diode beam blocked or unblocked. In order to calculate the susceptibility for the metastable state, we have to divide the blue signal by the visible pumping power:

$$\chi_{exp} = \Delta_{signal}/(P_{dye}\Delta P_{diode})$$

where Δ_{signal} is the blue enhancement intensity due to the diode beam, and P_{dye} and ΔP_{diode} are the diode and dye laser power, respectively. The results are presented in Fig. 2. Firstly, it can be seen that there is a significant increase of the susceptibility around the threshold which is characteristic of a bifurcation phenomenon (Curie law). Secondly, as the susceptibility is larger below the threshold than above, it implies that the GSA has no significant impact on the fluorescence intensity once the pumping threshold is surpassed.

Table 4
Comparison of the photon avalanche experimental results for YAG: 5 at% Tm^{3+} at 35 K under 638 or 617 nm excitation

	YAG (exc: 638 nm)	YAG (exc: 617 nm)
$\eta(s_4)$ (%)	91	91
$\eta(s_3)$ (%)	96	96
τ_2 (ms)	12	12
R_{2th} (s^{-1})	49.5	49.5
I_{th} (kW cm^{-2})	11.3	1.9
n_{th}	3.5	6
τ_e/τ_2	7	25
σ_2 (10^{-20} cm^2)	0.13	0.85
σ_1/σ_2	6×10^{-3}	0.5×10^{-3}

4. Conclusion

Based on theoretical results, it is clear that the efficiency of the photon avalanche depends on three fundamental parameters: the cross relaxation rates, the ratio of the nonresonant GSA to the resonant ESA cross sections and the metastable state lifetime. Experimentally, by using different rare-earth concentrations, different excitation wavelengths or different hosts for the active ion, we have found that these parameters act on the photon avalanche as predicted by the theory. So, with the help of our reliable model [2] for predicting efficient photon avalanche upconversions, and thanks to the development of rare-earth-doped crystalline waveguides, which combine high emission cross section of crystals with a confinement and

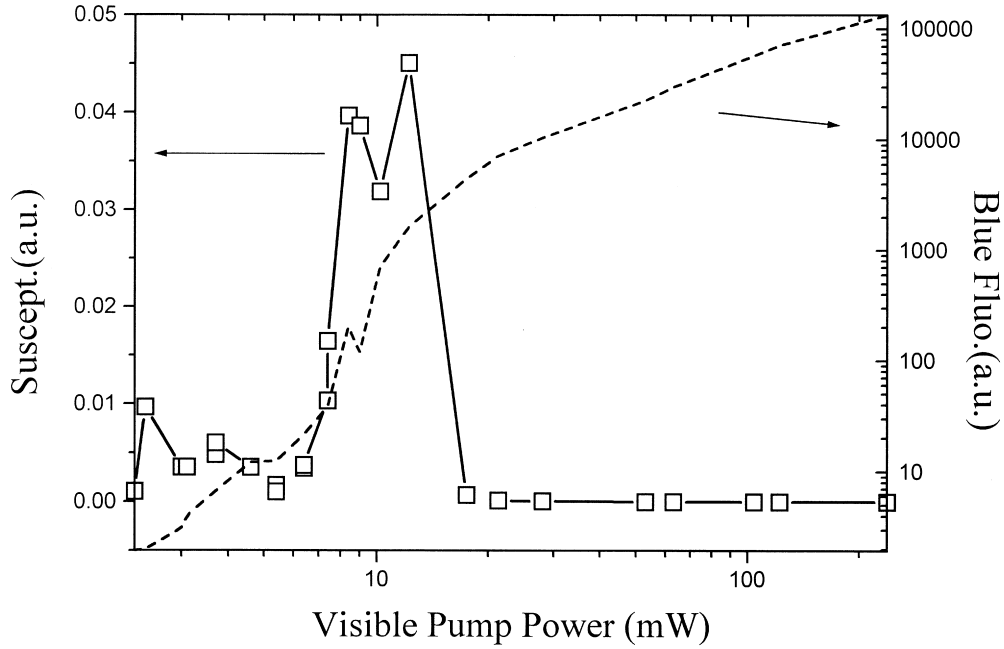

Fig. 2. Visible laser power dependence of the upconverted blue fluorescence and of the susceptibility in YLF: 1.8 at% Tm^{3+} at room temperature.

guiding effect, we believe that the photon avalanche is a promising route for future short wavelength microsources.

Acknowledgements

The authors thank M. Malinowski from Warsaw University of Technology, Poland, A. Tkachuk from the S.I. Vavilov State Optical Institute, Russia, R.M. Macfarlane from Almaden Research Center, California, R. Moncorgé from the UMR CNRS 5620 and J.L. Adam from the URA CNRS 442, France, for providing the samples used in this work.

References

[1] J.S. Chivian, W.E. Case, D.D. Eden, Appl. Phys. Lett. 35 (1979) 124.
[2] S. Guy, M.-F. Joubert, B. Jacquier, Phys. Rev. B 55 (1997) 8420.
[3] H. Ni, S.C. Rand, Opt. Lett. 16 (1991) 1424.
[4] T. Hebert, R. Wannemacher, R.M. Macfarlane, W. Lenth, Appl. Phys. Lett. 60 (1992) 2592.
[5] S. Guy, M.-F. Joubert, B. Jacquier, Phys. Status Solidi (b) 183 (1994) K33.
[6] M.F. Joubert, S. Guy, C. Linarès, B. Jacquier, J. Non-Cryst. Solids 184 (1995) 98.
[7] C. Borel, A. Rameix, Ph. Thony, B. Ferrand, D.P. Shepherd, A.C. Large, T.J. Warburton, A.C. Tropper, D.C. Hanna, S. Guy, B. Jacquier, M.F. Joubert, in: B.H.T. Chai, S.A. Payne (Eds.), OSA Proceedings on Advanced Solid State Lasers, Vol. 24, Optical Society of America, Washington, DC, 1995, p. 37.
[8] S. Guy, D.P. Shepherd, M.F. Joubert, B. Jacquier, H. Poignant, J. Opt. Soc. Am. B 14 (1997) 926.
[9] Ph. Goldner, F. Pellé, Opt. Mater. 5 (1996) 239.
[10] N. Garnier, R. Moncorgé, Y. Guyot, E. Descroix, H. Manaa, P. Laporte, Ann. Chim. Fr. 20 (1995) 249.